

# Temperature Dependence of NQR Spectra and Phase Transitions in Alkali Metal Hexaiodozirconates and Hafnates (IV)\*

E. A. Kravchenko, V. G. Morgunov, Z. B. Mukhametshina, V. V. Chibrikina, and G. A. Yagodin

Institute of General and Inorganic Chemistry, Academy of Sciences of the USSR, Moscow

Z. Naturforsch. **41a**, 294–298 (1986); received July 20, 1985

Hexaiodometallates of the type  $R_2MI_6$  ( $R = \text{Li, Na, K, Rb, Cs}$ ;  $M = \text{Zr, Hf}$ ) have been studied over a wide temperature region using  $^{127}\text{I}$  NQR. They show a notable diversity of structures. The values of the  $^{127}\text{I}$   $e^2Qq/h$  in hafnates appeared to exceed those in related zirconates by about 10%. This, together with the more positive temperature coefficients of the NQR spectra in zirconates is accounted for by a slightly greater  $\pi$ -character in the  $\text{Zr}-\text{I}$  than the  $\text{Hf}-\text{I}$  bonds in related compounds. Several 1st and 2nd order phase transitions have been detected in  $\text{Na}_2\text{MI}_6$  (I) and  $\text{Rb}_2\text{MI}_6$  (II). In (I) the high-temperature phase has a structure of lower symmetry than the low-temperature phase, and the 1st order phase transition point reveals an extremely large range of hysteresis.

## Introduction

Much information obtained using NQR on hexahalometallates of Groups VI–VIII transition metals is now available and has been reviewed [1–3]. Crystal and electronic structures, lattice dynamics and phase transitions (PT) have been extensively studied in a number of compounds. This paper gives the results of a  $^{127}\text{I}$  NQR study on previously unknown hexahalometallates (IV), namely alkali metal hexaiodozirconates and hafnates (IV)\* carried out over a wide range of temperatures.

## Experimental

The preparation of several title compounds has been described earlier [4, 5]. The remaining salts were prepared similarly. The temperature of the reaction zone varied from compound to compound; it was firstly raised to the melting point of the salt (or to the point of peritectic conversion of the Na salts, melting incongruently) and then allowed to fall to 20–50° below this point, at which level it was maintained for approximately 30 min. All manipulations excluded contact of the reactants with air moisture. Some of the compounds were analyzed

using DTA and XPA. NQR measurements have been carried out using a pulse spectrometer operating within the range 10–300 MHz (SKB IRE AN SSSR).

## Results and Discussion

The  $^{127}\text{I}$  NQR data of the compounds studied are listed in Table I for several temperatures. Some of them are seen to change multiplicity with temperature. Hence we have studied the temperature dependence of the  $^{127}\text{I}$  transition frequencies and derived the values of  $e^2Qq/h$  (QCC) (Figures 1–4). The results indicate that both pairs,  $\text{Li}_2\text{MI}_6$  and  $\text{Cs}_2\text{MI}_6$  ( $M = \text{Zr, Hf}$ ), form regular  $[\text{MI}_6]^{2-}$  octahedra at all temperatures studied, the spectral singlets showing a linear dependence on temperature with positive coefficients (Figure 1). The latter are evidently greater in the Zr than in the Hf salts. According to XPA the salts  $\text{Li}_2\text{MI}_6$  crystallize in a body-centered cubic  $\text{Im } 3m$  lattice with unit cell dimensions  $a = 13.61$  and  $13.57 \text{ \AA}$  for the Zr and Hf respectively. Both  $\text{Cs}_2\text{MI}_6$  salts have a body-centered cubic  $\text{Fm } 3m$  lattice,  $a = 11.613 \text{ \AA}$  in  $\text{Cs}_2\text{ZrI}_6$  and  $a = 11.609 \text{ \AA}$  in  $\text{Cs}_2\text{HfI}_6$  [4, 6], with a bonding distance  $\text{Hf}-\text{I} = 2.829(2) \text{ \AA}$  and an interatomic distance  $\text{Cs}-\text{I} = 4.105(1) \text{ \AA}$  [6].

$\text{Na}_2\text{ZrI}_6$  and  $\text{Na}_2\text{HfI}_6$  give singlet NQR spectra at low temperatures only (Figure 2). On heating the Zr salt to +65 °C and the Hf salt to +90 °C, a 1<sup>st</sup> order phase transition (PT) occurs with discontinuities in the temperature curves. The spectra of the high-temperature (HT) phases appear with a large split-

\* Communicated to the VIIIth International Symposium on Nuclear Quadrupole Resonance Spectroscopy, Darmstadt, July 22–26, 1985.

Reprint requests to Mrs. Dr. E. A. Kravchenko, Institute of General and Inorganic Chemistry, Leninskii Pr. 31, 117907, GSP-I, Moscow V-907, USSR.

0340-4811 / 86 / 0100-0294 \$ 01.30/0. – Please order a reprint rather than making your own copy.



Dieses Werk wurde im Jahr 2013 vom Verlag Zeitschrift für Naturforschung in Zusammenarbeit mit der Max-Planck-Gesellschaft zur Förderung der Wissenschaften e.V. digitalisiert und unter folgender Lizenz veröffentlicht: Creative Commons Namensnennung-Keine Bearbeitung 3.0 Deutschland Lizenz.

Zum 01.01.2015 ist eine Anpassung der Lizenzbedingungen (Entfall der Creative Commons Lizenzbedingung „Keine Bearbeitung“) beabsichtigt, um eine Nachnutzung auch im Rahmen zukünftiger wissenschaftlicher Nutzungsformen zu ermöglichen.

This work has been digitalized and published in 2013 by Verlag Zeitschrift für Naturforschung in cooperation with the Max Planck Society for the Advancement of Science under a Creative Commons Attribution-NoDerivs 3.0 Germany License.

On 01.01.2015 it is planned to change the License Conditions (the removal of the Creative Commons License condition “no derivative works”). This is to allow reuse in the area of future scientific usage.

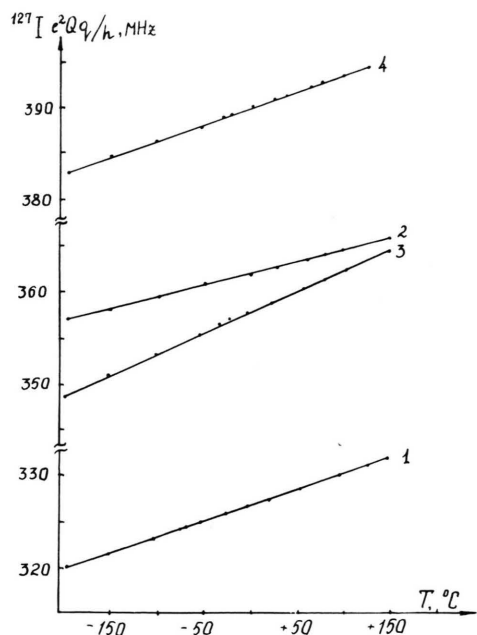


Fig. 1. Temperature dependence of the  $^{127}\text{I}$  quadrupole coupling constants ( $e^2Qq/h$ ) in the compounds:  $\text{Li}_2\text{ZrI}_6$ —1;  $\text{Li}_2\text{HfI}_6$ —2;  $\text{Cs}_2\text{ZrI}_6$ —3;  $\text{Cs}_2\text{HfI}_6$ —4.

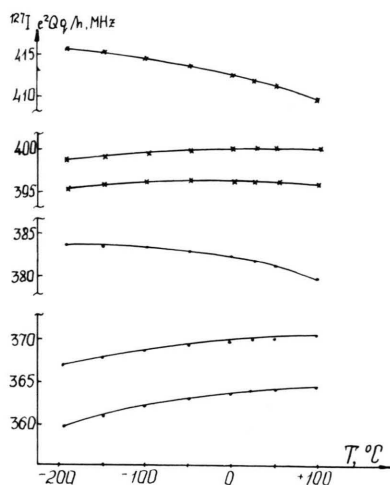


Fig. 3. Temperature dependence of the quadrupole coupling constants ( $^{127}\text{I}$   $e^2Qq/h$ ) in  $\text{K}_2\text{ZrI}_6$  (circles) and  $\text{K}_2\text{HfI}_6$  (crosses).

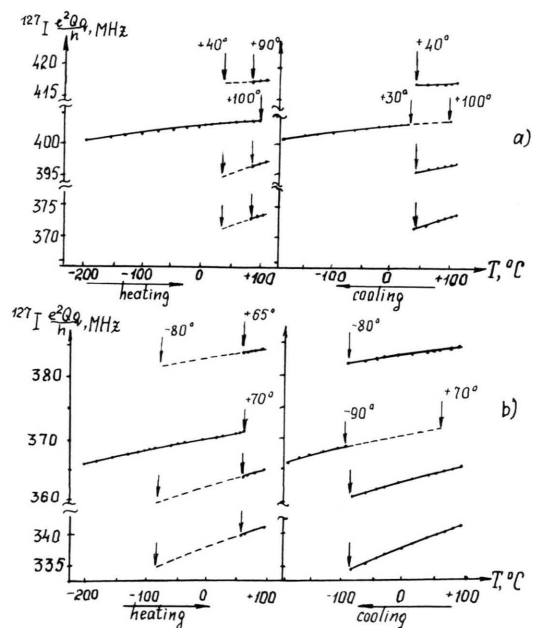


Fig. 2. Temperature dependence of the  $^{127}\text{I}$  quadrupole coupling constants ( $e^2Qq/h$ ) in  $\text{Na}_2\text{HfI}_6$  (a) and  $\text{Na}_2\text{ZrI}_6$  (b) on heating (left) and on cooling (right). The dotted lines show the range of hysteresis.

ting and increased asymmetry parameters  $\eta$  [7]. NQR displays in this case a rare situation when the HT phase has a structure of lower symmetry (presumably monoclinic) than the low-temperature (LT) phase. If a temperature run is reversed, starting from +100 °C, the HT resonances exist in  $\text{Na}_2\text{ZrI}_6$  down to -80 °C while those of the LT phase reappear at -90 °C only, revealing an extremely large hysteresis of the PT point. The temperature changes of  $\text{Na}_2\text{HfI}_6$  are of similar type but show a smaller range of hysteresis.  $\text{K}_2\text{ZrI}_6$  and  $\text{K}_2\text{HfI}_6$  give split  $^{127}\text{I}$  NQR spectra (Table 1) showing inequivalence of the M—I bonds in the  $[\text{MI}_6]^{2-}$  anions due to their distortion. The preliminary XPA data show a symmetry not higher than monoclinic in both salts. The distortion of the octahedra might be caused by interionic interactions associated with elongation of the corresponding M—I bonding distances. Since the  $d^0$  configuration of the complexes assumes vacancies in their  $d_e^*$  orbitals suitable for accepting  $p_\pi$  electron density from halogens, the elongation of the M—I bond is expected to reduce its  $p_\pi$ - $d_\pi$  character. This, according to the Townes and Dailey theory [8], will shift the corresponding  $^{127}\text{I}$  resonance to higher frequencies with respect to those displayed by the atoms not disturbed by interionic interactions. The other spectral evidence for interionic contacts is provided by the temperature dependence. The relatively increased  $\sigma$ -character of

Table 1.  $^{127}\text{I}$  NQR spectra of alkali metal hexaiodozirconates and hafnates (IV).

R	T, K	Compounds of the type $\text{R}_2\text{ZrI}_6$				Compounds of the type $\text{R}_2\text{HfI}_6$			
		Transition freqs. (MHz)		$e^2Qq/h$ (MHz)	$\eta$ (%)	Transition freqs. (MHz)		$e^2Qq/h$ (MHz)	$\eta$ (%)
		1/2–3/2	3/2–5/2			1/2–3/2	3/2–5/2		
Li	77	48.15	96.03	320.2	4.7	53.65	107.08	357.0	4.0
	300	49.29	98.17	327.4	5.8	54.52	108.68	362.2	5.5
Na	77	55.00	109.79	366.1	3.9	60.27	120.23	400.9	4.5
	300 <sup>a</sup>	55.67	111.10	370.4	4.0	60.66	120.96	403.4	4.7
	300 <sup>b</sup>	51.69	101.08	338.35	13.1				
		62.51	106.05	363.15	38.1				
		65.50	111.95	383.0	37.5				
K	77	55.32	107.51	359.8	14.0	60.40	118.22	395.2	13.1
		56.71	109.52	366.8	16.4	61.25	119.10	398.7	14.9
		61.96	113.33	383.3	27.2	66.32	123.28	415.6	24.5
	300	55.25	108.85	363.1	10.8	60.17	118.61	396.1	10.1
		56.70	110.52	369.8	14.1	61.01	119.62	400.0	12.8
		60.11	113.42	381.6	21.7	64.32	122.61	411.8	19.5
Rb	77	53.38	106.57	355.1	4.3	58.30	116.315	387.9	4.3
		55.16	106.82	357.5	16.3	59.96	116.73	390.75	14.6
		56.02	108.04	362.1	17.1	60.75	118.95	395.0	15.3
	300	52.84	105.61	352.0	2.4	58.22	115.68	386.0	7.2
		53.75	106.25	354.9	9.5	57.25	114.52	381.7	0.0
	373	52.40	104.73	349.1	0.0	57.12 <sup>c</sup>	114.14 <sup>c</sup>	380.5 <sup>c</sup>	2.6 <sup>c</sup>
Cs	77	52.29	104.53	348.5	1.9	57.71	114.99	383.0	4.3
	300	53.85	107.69	359.0	0.8	58.74	117.40	391.4	0.0

<sup>a</sup> After cooling to 77 K; <sup>b</sup> After heating above +65 °C; <sup>c</sup> At 403 K.

the elongated bond will evidently produce a negative contribution to the temperature coefficient of this line.

As one can see from Fig. 3, one of the  $^{127}\text{I}$  signals is shifted to higher frequencies with respect to the doublet, and its temperature dependence is negative, in contrast to the positive temperature coefficients of the doublet lines. This, as well as the larger values of  $\eta$  for the high-frequency singlets supports the suggestion of interionic interactions in the potassium salts. **Rb<sub>2</sub>ZrI<sub>6</sub>** and **Rb<sub>2</sub>HfI<sub>6</sub>** undergo several phase transitions (Figure 4). Two weak endothermal peaks have been observed (–18 °C, +81 °C in the Zr salt; –23 °C, +81 °C in the Hf salt) on their DTA curves [9]. NQR confirms these results and reveals one more PT near room temperature (PT-3 in Figure 4). It is characterized by a change in the  $d(\text{QCC})/dT$  value. The PT's of similar appearance observed at –16 °C in **K<sub>2</sub>ReBr<sub>6</sub>** (Fig. 5a) and at –52 °C in **K<sub>2</sub>SeBr<sub>6</sub>** have been accounted [1] for by torsional oscillations of the  $[\text{MBr}_6]^{2-}$  ions about one of the M–Br axes, so that the corresponding resonances are insensitive to the PT. In the **RbMI<sub>6</sub>** com-

pounds the nature of PT-3 might be similar but the axes of torsional oscillations can hardly coincide with any of the M–I bonding directions since all the spectral lines are sensitive to this PT.

A great number of  $\text{R}_2\text{MX}_6$  antiferroite compounds are at present known [2] which show NQR temperature dependences resembling those in Figure 4. Thus, compounds like **Rb<sub>2</sub>MI<sub>6</sub>**, **K<sub>2</sub>SnBr<sub>6</sub>** and **K<sub>2</sub>TeBr<sub>6</sub>** have three component NQR spectra in their LT phases [2], indicating a symmetry of the crystals lower than tetragonal. Indeed it is monoclinic in **K<sub>2</sub>TeBr<sub>6</sub>** with a space group  $\text{P}2_1/n$  [10]. Above the low-temperature PT point, **Rb<sub>2</sub>MI<sub>6</sub>** gives two-component spectra, the symmetry of the salts becoming tetragonal with probable space group  $\text{P}4/\text{nc}$  or  $\text{P}4/\text{mnc}$  and unit cell dimensions  $a = 8.090$ ,  $c = 11.771$  Å and  $a = 8.076$ ,  $c = 11.673$  Å for the Zr and Hf salts, respectively.

In the known antiferroite compounds, a tetragonal phase appears on cooling the cubic **K<sub>2</sub>PtCl<sub>6</sub>**-type crystals below the PT point. The PT involves, as in **K<sub>2</sub>ReCl<sub>6</sub>**, a gradual rotation of the  $[\text{MX}_6]^{2-}$  anions through a small angle  $\theta$  around the  $z$  axis [11]

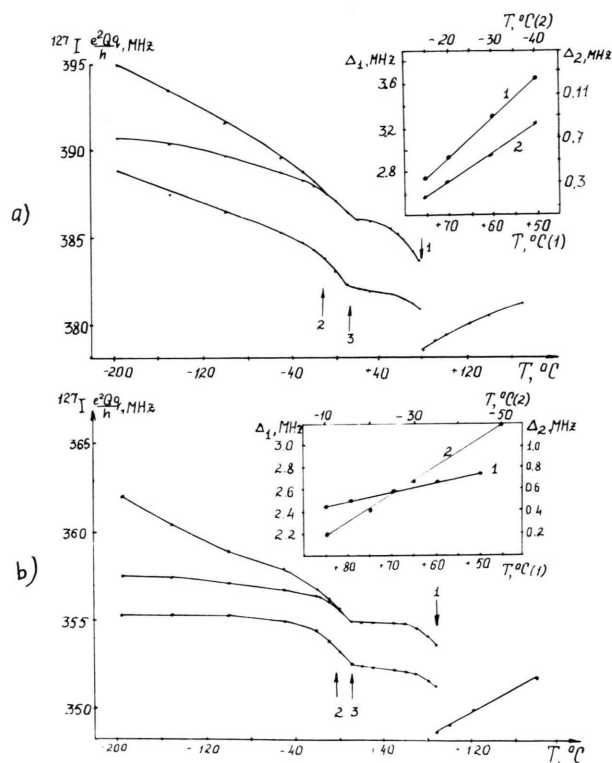


Fig. 4. Temperature dependence of the  $^{127}\text{I}$  quadrupole coupling constants ( $e^2Qq/h$ ) in  $\text{Rb}_2\text{ZrI}_6$  (a) and  $\text{Rb}_2\text{HfI}_6$  (b). Arrows show the phase transition (PT) points. In the inserts, the temperature dependence of the spectral splitting ( $\Delta = e^2Qq_1/h - e^2Qq_2/h$ ) below the PT-1 ( $\Delta_1$ ) and PT-2 ( $\Delta_2$ ) is shown. Above PT-2  $\Delta_2 = 0$ .

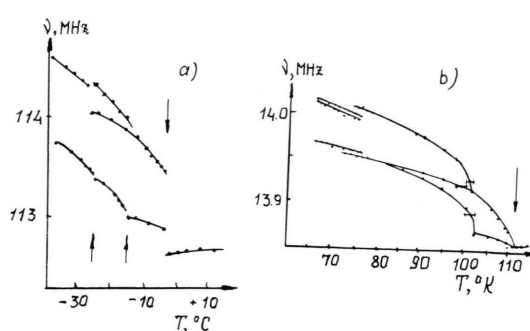


Fig. 5. a) Temperature dependence of  $^{79}\text{Br}$  NQR frequencies in  $\text{K}_2\text{ReBr}_6$  [1]. Arrows show the phase transition (PT) points. b) Temperature dependence of  $^{35}\text{Cl}$  NQR frequencies in  $\text{K}_2\text{ReCl}_6$  [11]. Arrow shows the PT point from the cubic to tetragonal phase.

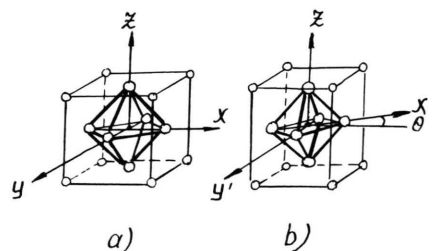


Fig. 6. Orientation of the  $[\text{ReCl}_6]^{2-}$  anions in the cubic (a) and tetragonal (b) modifications of  $\text{K}_2\text{ReCl}_6$  [2].

(Figure 6). The NQR signal observed in the cubic phase undergoes only a slight frequency shift below the PT point (Fig. 5b). The octahedra remain undistorted in the LT phase that is characterized by small tetragonal distortion of the R cation cage. The mechanism of the PT in  $\text{K}_2\text{ReCl}_6$  was attributed [11] to a soft rotary mode of the  $[\text{ReCl}_6]^{2-}$  anion, the force constant of which is markedly temperature dependent and vanishes at the PT point. It was also shown in NQR temperature dependence studies of antiferrofluorites [3, 12] that  $\Delta\nu \sim A\theta^2$ , where  $\Delta\nu$  is the spectral splitting several degrees below the PT point and  $A$  is constant. From the other side, the linear temperature dependence of  $\Delta\nu$  within several degrees below the PT (Fig. 5b) indicates that  $\theta \sim (T - T_0)^{1/2}$ , in agreement with the Landau theory,  $\theta$  being the order parameter. Using this approach,  $\theta$  is estimated to be about  $4^\circ$  in  $\text{K}_2\text{ReCl}_6$ ,  $7^\circ$  in  $\text{K}_2\text{PtBr}_6$  and  $11^\circ$  in  $(\text{NH}_4)_2\text{PtBr}_6$  [3].

It is to be noted that the octahedra remain undistorted not only in the tetragonal phase but also in the phases with symmetries lower than tetragonal [10, 12]. In the monoclinic phase of  $\text{K}_2\text{TeBr}_6$ , the  $[\text{TeBr}_6]^{2-}$  octahedra are reported [10] to be regular ( $O_h$ ), each being rotated through small angles successively around two axes of the unit cell.

One can therefore conclude that a displacive PT of 2nd order, when identified by NQR, is characterized by a temperature dependence of the spectra showing no appreciable discontinuity at the PT point with a spectral splitting varying linearly with temperature within a few degrees below the PT point.

As Fig. 4 shows, these very features characterize the low-temperature PT (PT-2) in both Rb salts. The high-temperature PT (PT-1) shows however a slight discontinuity indicating that volume effects,  $\pi$ -bonding effects, etc. might contribute to the

Table 2. The M–I chemical bond characters  $i$ ,  $\sigma$ ,  $\pi$  and temperature coefficients of the quadrupole coupling constants ( $e^2 Qq/h$ ) in the high-symmetry phases of alkali metal hexaiodozirconates and hafnates (IV) according to  $^{127}\text{I}$  NQR.

Compounds of the type $\text{R}_2\text{ZrI}_6$					Compounds of the type $\text{R}_2\text{HfI}_6$				
$R$	$i$	$\sigma$	$\pi$	$\frac{d(e^2 Qq/h)}{dT}$ (kHz/deg.)	$i$	$\sigma$	$\pi$	$\frac{d(e^2 Qq/h)}{dT}$ (kHz/deg.)	
Li	0.21	0.356	0.434	+33.7	0.20	0.371	0.429	+24.9	
Na	0.21	0.370	0.420	+18.8	0.20	0.383	0.417	+9.8	
Rb	0.21	0.365	0.425	+49.2	0.20	0.377	0.423	+41.0	
Cs	0.21	0.365	0.425	+45.7	0.20	0.378	0.422	+35.0	

change in EFG at the PT point [3]. But the temperature behaviour of the spectral splitting below the PT point resembles that in antiferrofluorites (see inserts in Fig. 4), allowing one to think that this PT also occurs from a cubic phase and involves rotation of the  $[\text{MI}_6]^{2-}$  octahedra.

Summarizing the results obtained, we must note that the  $^{127}\text{I}$  QCC values in all the hafnates appear to exceed those in related zirconates by about 10% (Table 1), although the Zr and Hf atoms have very similar atomic ( $R_{\text{Zr}} = R_{\text{Hf}} = 1.55$ ) and ionic ( $\text{Zr}^{+4} = 0.79$ ;  $\text{Hf}^{+4} = 0.78$ ) radii and electronegativities ( $\chi_{\text{Zr}} = 1.22$ ;  $\chi_{\text{Hf}} = 1.23$ ) [13]. Since Figs. 1–4 show the positive temperature coefficients of the  $^{127}\text{I}$  QCC values to be greater in the Zr than in the Hf salts, we assume that these differences originate partly from the relatively higher  $\pi$ -character of the Zr–I than the Hf–I bonds in related pairs. In order to get a quantitative view of the extent of the variation in bonding parameters sufficient to produce the observed differences in the QCC values, we have calculated within the approximations of the Townes and Dailey theory [8] the M–I bonding character in the high-symmetry modifications of the compounds

studied (Table 2). The extents of ionic,  $\sigma$ -covalent and  $\pi$ -covalent character are denoted by  $i$ ,  $\sigma$  and  $\pi$ , respectively. Assuming that  $i + \sigma + \pi = 1$ ,  $\pi_x + \pi_y = \pi$ , and neglecting  $s$ -hybridization of the  $\sigma$ -bonding orbitals, we have

$$\frac{e^2 Qq}{e^2 Qq_{\text{at}}} = \frac{N_x + N_y}{2} - N_z = \sigma - \frac{\pi_x + \pi_y}{2} = \sigma - \frac{\pi}{2} = 1 - i - \frac{3}{2}\pi.$$

Here  $N_j$  ( $j = x, y, z$ ) are the occupancies of the valence  $p_j$  orbitals on the iodine atom. They are evidently equal to:  $N_z = 2 - \sigma$ ,  $N_x = 2 - \pi_x$ ,  $N_y = 2 - \pi_y$ ; we take  $e^2 Qq_{\text{at}}/h = 2292.7$  MHz [14]. The value of  $i$  was determined from electronegativity differences [13]. The reliability of the numerical values of  $i$ ,  $\sigma$ ,  $\pi$  so obtained is of course not high. They are however useful to show that the measured difference between the  $^{127}\text{I}$  QCC values in the related pairs of compounds can be produced by tiny variations in the M–I bonding parameters, the greater  $\pi$ -values of the Zr–I bonds relative to the Hf–I bonds contributing to the observed difference.

- [1] M. Kubo and D. Nakamura, *Adv. Inorg. Chem. Radiochem.* **8**, 257 (1966).
- [2] D. Nakamura, R. Ikeda, and M. Kubo, *Coord. Chem. Rev.* **17**, 281 (1975).
- [3] R. L. Armstrong and H. M. van Driel, *Adv. Nucl. Quadrupole Res.* **2**, 179 (1975).
- [4] V. V. Chibrikov, Z. B. Mukhametshina, V. P. Seleznev, and G. A. Yagodin, *Zh. Neorgan. Khim.* **25**, 3394 (1980).
- [5] Z. B. Mukhametshina, V. V. Chibrikov, V. P. Seleznev, and G. A. Yagodin, *Trudy MKhTI im. D. I. Mendeleeva; Khimia i Tekhnologia Redkikh i Rasseyanykh Elementov* **125**, 88 (1982).
- [6] D. Sinram, C. Brendel, and B. Krebs, *Inorg. Chim. Acta* **64**, 131 (1982).
- [7] Assignment of the NQR spectra is made in order of increasing frequencies. An alternative assignment does not change the conclusions.
- [8] C. H. Townes and B. P. Dailey, *J. Chem. Phys.* **17**, 782 (1949).
- [9] V. V. Chibrikov, Yu. V. Shabaev, Z. B. Mukhametshina, V. P. Seleznev, and G. A. Yagodin, *Zh. Neorgan. Khim.* **26**, 2560 (1981).
- [10] I. D. Brown, *Canad. J. Chem.* **42**, 2758 (1964).
- [11] G. P. O'Leary and R. G. Wheeler, *Phys. Rev.* **B1**, 4409 (1970).
- [12] H. M. van Driel, M. Wiszniewska, B. M. Moores, and R. L. Armstrong, *Phys. Rev.* **B6**, 1596 (1972); M. Wiszniewska, and R. L. Armstrong, *Canad. J. Phys.* **51**, 781 (1973).
- [13] M. C. Day, Jr. and J. Selbin, *Teoret. Neorgan. Khimia*, p. 135, Khimia, Moscow (1976).
- [14] V. Jaccarino, J. G. King, R. H. Satten, and H. H. Stroke, *Phys. Rev.* **94**, 1798 (1954).